

# RATE CONSTANTS FOR UNIMOLECULAR DECOMPOSITION OF SF<sub>6</sub><sup>-</sup>

Yicheng Wang,<sup>†</sup> R. L. Champion,<sup>‡</sup> I. V. Dyakov,<sup>‡</sup> and B. L. Peko<sup>‡\*</sup>

## 1. INTRODUCTION

Sulfur hexafluoride (SF<sub>6</sub>) is widely used as a gaseous dielectric in high-voltage applications due to its extremely large cross section for electron attachment [1-3] and the stability of SF<sub>6</sub><sup>-</sup> with respect to decomposition in subsequent collisions with SF<sub>6</sub> [4]. It is also recognized as a potent greenhouse gas and it has been suggested that a mixture of SF<sub>6</sub> and N<sub>2</sub> might serve as a substitute for pure SF<sub>6</sub> in certain applications which require gaseous dielectrics [5,6]. Even with a very low SF<sub>6</sub> content, a SF<sub>6</sub>/N<sub>2</sub> mixture exhibits many of the desirable properties of SF<sub>6</sub> as a gaseous dielectric. It has been suggested that this mixture may constitute a synergistic combination: the buffer gas (N<sub>2</sub>) serves to cool energetic electrons into the low-energy region where the electronegative gas (SF<sub>6</sub>) captures them with a remarkably high cross section, thereby inhibiting the buildup of free electrons that could cause ionization leading to electrical breakdown. The dielectric properties of this mixture have been the subject of numerous recent investigations [5,6].

Collisions of SF<sub>6</sub><sup>-</sup> with N<sub>2</sub> which result in the decomposition of SF<sub>6</sub><sup>-</sup> are obviously involved in such mixtures when used as gaseous insulators. Cross sections for electron attachment to SF<sub>6</sub> along with those associated with the decomposition of SF<sub>6</sub><sup>-</sup> can partially characterize the arc-quenching properties of the mixture, *viz.*, the ability of the mixture to capture free electrons and keep them bound in subsequent collisions. The collisional decomposition of SF<sub>6</sub><sup>-</sup> will also be an important reaction pathway leading to creation of chemical by-products and thus needs to be understood in order to fully characterize the

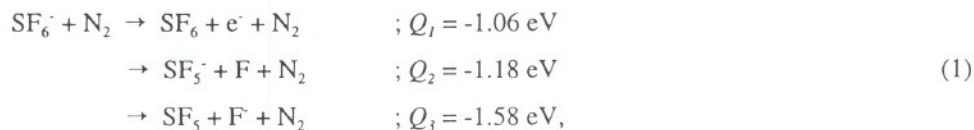
---

<sup>†</sup> National Institute of Standards and Technology, Gaithersburg, MD 20899-8113, USA

<sup>‡</sup> College of William and Mary, Williamsburg, VA 23187, USA

\* present address: Dept. of Physics, University of Denver, 2112 E. Wesley Ave., Denver, CO 80208

dielectric and chemical stability of SF<sub>6</sub>/N<sub>2</sub> mixtures. The purpose of this paper is to report rate constants for collision-induced decomposition of SF<sub>6</sub><sup>-</sup> for the following three least endothermic reactions:



where the threshold energies for each channel,  $Q_i$  ( $i = 1, 2, 3$ ), are for ground state reactants and products [7,8]. The decomposition of SF<sub>6</sub><sup>-</sup> is modeled with a two-step mechanism in which collisional excitation of SF<sub>6</sub><sup>-</sup> to SF<sub>6</sub><sup>-\*</sup> is followed by unimolecular decomposition of SF<sub>6</sub><sup>-\*</sup>. Unimolecular decomposition rates are based on recent thermochemical data and a statistical model first proposed by Klots [9]. The model results will be compared with the recently measured total cross sections for electron detachment and collision-induced dissociation (CID) for SF<sub>6</sub><sup>-</sup> + N<sub>2</sub> [10].

## 2. MODEL

Recent cross section measurements for electron detachment and CID of SF<sub>6</sub><sup>-</sup> by N<sub>2</sub> [10] show that although electron detachment has the lowest threshold energy for decomposition, CID is the dominant decomposition mechanism for the anion, except for the lowest collision energies. The CID channel leading to the production of F<sup>-</sup> has a higher energetic threshold than that for SF<sub>5</sub><sup>-</sup>, which may be attributed to its lower electron affinity. The electron detachment cross section exhibits a minimum for a relative collision energy around 25 eV and increases sharply thereafter. These features are strikingly similar to previous observations for collisions of SF<sub>6</sub><sup>-</sup> with rare gases. Such target-independent results are often described by a two-step mechanism where collisional excitation of SF<sub>6</sub><sup>-</sup> by the target X is followed by its unimolecular decomposition; viz.,



where  $U$  is the total internal energy of the unstable, excited SF<sub>6</sub><sup>-\*</sup> product which is partitioned rovibrationally, and  $J_o$  is the rotational quantum number, indicating that portion of  $U$  which is rotational energy.

The overall dominance of CID over electron detachment for collision energies where all the reaction channels are energetically accessible can be qualitatively understood with the help of the unimolecular decomposition model originally proposed by Klots [9,11]. In this model, the decomposition rates of SF<sub>6</sub><sup>-\*</sup> for products given in (1) may be expressed by

$$k_i(U, J_o) = \frac{\beta_i}{h(2J_o+1)\rho_{\text{vib}}^{(\text{SF}_6^-)^*}(E_{\text{vib}})} \times \int_{\epsilon=0}^{U_i=U-Q_i} \rho_{\text{vib}}^{\text{product}}(\epsilon) \sum_J \sum_L (2J+1) d\epsilon, \tag{3}$$

assuming that  $(\text{SF}_6^-)^*$  and polyatomic products of its decomposition can be treated as spherical tops. In the expression above  $\rho_{vib}$  is the vibrational density of states,  $J$  is the rotational angular momentum of the product spherical top,  $L$  is the orbital angular momentum of the products,  $\beta_i$  is the ratio of the symmetry numbers of  $(\text{SF}_6^-)^*$  and the product spherical top. The vibrational density of states can be approximated [12] as

$$\rho_{vib}(\epsilon) = \frac{(\epsilon + \epsilon_0)^{s-1}}{(s-1)! \prod_{i=1}^s h\nu_i}, \quad (4)$$

where  $\epsilon_0$  is the zero-point energy,  $\epsilon$  is the energy above the zero-point level,  $s$  is the number of vibrational degrees of freedom, and  $\nu_i$  are the vibrational frequencies. It is not necessary to consider excited electronic states of the anion in this treatment as, for a given  $U$ , the vibrational density of states of any excited electronic state will be negligible compared to that for the ground state.

To evaluate (4), the values of vibrational frequencies  $\nu_i$  for  $\text{SF}_6^-$ ,  $\text{SF}_6$ ,  $\text{SF}_5^-$  and  $\text{SF}_5$  were taken from recent calculations by Lugez *et al.* [13]. Not all of these vibrational frequencies are known experimentally. Where both the calculated and experimentally determined frequencies exist ( $\text{SF}_6$ , for example), their differences are in the range of 10%. It is important to point out that a change of this magnitude for  $\nu_i$  does not alter the conclusions which arise from these calculations in any substantive manner.

The internal energy,  $U$ , of  $(\text{SF}_6^-)^*$  was assumed to partition equally among its three rotational and fifteen vibrational degrees of freedom. The initial angular momentum quantum number,  $J_0$ , was then calculated according to

$$E_{rot} = B J (J+1) \quad (5)$$

for a spherical top where  $B$  is the rotational constant. The threshold energies,  $Q_i$ , for electron detachment and CID into  $\text{SF}_5^-$  or  $\text{F}$  given in (1) were used in the calculation. There exist some uncertainties about these threshold energies, but there is a general agreement on the order in which these values follow [7,8].

The restrictions on the product angular momentum quantum numbers  $J$  and  $L$  in (3) were determined as follows: For electron detachment, s-electrons dominate the detachment mechanism or  $L = 0$  and  $J = J_0$ . For CID channels 2 and 3, once a value of  $\epsilon$  is chosen, the rotational energy,  $E_{rot}$ , of the product spherical top can range from zero to  $U - Q_i - \epsilon$ . The range of  $J$  is then calculated according to Eq. (5). Two factors determine the range of  $L$  in (3): the triangle rule  $|J - J_0| \leq L \leq J + J_0$  and the Langevin orbiting restriction [9]

$$L_{max}(L_{max}+1) = \gamma(U - Q_i - \epsilon - E_{rot}).$$

Here,

$$\gamma = 2^{3/2} \mu e \alpha^{1/2} / \hbar^2,$$

where  $\mu$  is the reduced mass of the CID products, and  $\alpha$  is the polarizability of the neutral product. In these calculations we assumed that  $\text{SF}_5^-$ , when its internal energy is high enough, would itself decompose. The decomposition channel for  $\text{SF}_5^-$  which has the lowest threshold energy is  $\text{F}^- + \text{SF}_4$  (1.1 eV) [13]. The threshold energies for decomposing into  $\text{SF}_4^- + \text{F}$  (3.0 eV) and  $\text{e}^- + \text{SF}_5$  (3.8 eV) [13] are significantly higher and, as will become clear later in this paper, they are beyond the energy range of the present treatment. The decomposition rate,  $k_4$ , for  $\text{SF}_5^- \rightarrow \text{F}^- + \text{SF}_4$  was calculated using the same statistical model, with vibrational frequencies also taken from the work of Lugez *et al* [13]. The decomposition of  $\text{SF}_5^-$  produces a source for  $\text{F}^-$  and a sink for  $\text{SF}_5^-$ . The production rate of  $\text{F}^-$  via  $\text{SF}_5^-$  is governed by the rate of the slower, rate-determining step of the overall reaction, with a characteristic time  $\tau = 1/k_2 + 1/k_4$ . The combined effective rate for  $\text{F}^-$  production from  $(\text{SF}_6^-)^*$  is then  $k_3^{\text{eff}} = k_3 + 1/\tau$ , and for  $\text{SF}_5^-$  production, it is  $k_2^{\text{eff}} = k_2 - 1/\tau$ . Of course,  $k_1^{\text{eff}} = k_1$ , as we have considered no additional source or sink of electrons.

### 3. RESULTS AND DISCUSSION

The resulting decomposition rates for  $(\text{SF}_6^-)^*$  are presented in Figure 1. The main features which can be immediately observed are as follows. The decomposition rates for the three channels in Eq. (1) have onsets in the order of their internal threshold energies. However, the rates for the CID channels initially rise more steeply with increasing internal energy of  $\text{SF}_6^-$  than the detachment rate, which can be attributed to the larger phase space for the angular momenta of the CID products than that for the detachment products. The production of  $\text{SF}_5^-$  by CID becomes the dominant decay mechanism as  $U$  increases above 1.5 eV until it reaches around 2.3 eV where the secondary decomposition rate of  $\text{SF}_5^-$  rises so steeply that  $\text{F}^-$  quickly becomes the dominant product ion.

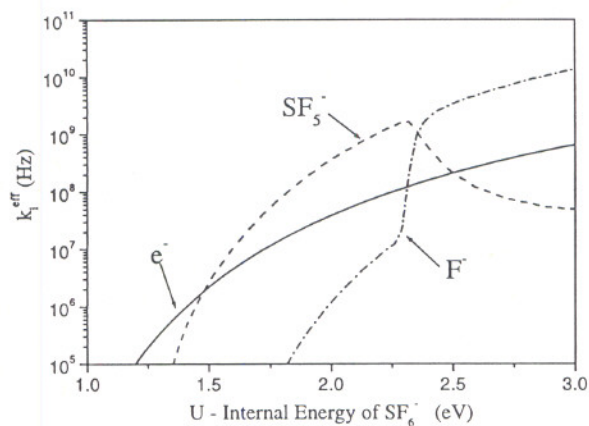


**Figure 1.** Calculated decomposition rates,  $k_1$ ,  $k_2^{\text{eff}}$ , and  $k_3^{\text{eff}}$ , are plotted as a function of the internal energy,  $U$ , of  $(\text{SF}_6^-)^*$ .

To facilitate comparison between the decomposition rates of  $(\text{SF}_6^-)^*$  and the decomposition cross sections in collisions of  $\text{SF}_6^-$  with  $\text{N}_2$ , we present the calculated branching ratios  $k_i^{\text{eff}}/(\sum k_i^{\text{eff}})$  as a function of  $U$  in Fig. 5(a) along with the recently measured branching ratios,  $\sigma_i/\sum(\sigma_i)$ , of the corresponding cross sections as a function of the relative collision energy,  $E_{\text{rel}}$ , in Fig. 5(b) [13]. As can be seen in the figure, the overall features of the calculated branching ratios resemble the experimentally determined branching ratios; both show that there are three distinct energy regions with different dominant product ions. This comparison clearly shows that the model calculation can be used to better understand the experimental results. As the collision energy increases, more translational energy is converted into the internal rovibrational excitation energy of  $(\text{SF}_6^-)^*$ . The first energetically allowed decomposition channel for  $(\text{SF}_6^-)^*$  is the electron detachment. The detachment probability quickly decreases, however, as the collision energy increases because the rate for the competing CID channel leading to  $\text{SF}_5^- + \text{F}$  rises faster. As  $U$  is increased further,  $\text{SF}_5^-$  becomes the dominant product ion in the intermediate energy region. The calculation also reveals that the decomposition rate for  $\text{SF}_5^- \rightarrow \text{F}^- + \text{SF}_4$  rises steeply as the internal energy increases above its decomposition threshold and this secondary process may, in fact, be the main source of  $\text{F}^-$  ions detected in collisions of  $\text{SF}_6^-$  with  $\text{N}_2$ . The statistical model can not, however, explain why the detachment cross section,  $\sigma_1(E_{\text{rel}})$ , rises for  $E_{\text{rel}} \geq 30$  eV. This increase observed for  $\sigma_1(E_{\text{rel}})$  is undoubtedly due to a competing, direct detachment mechanism which is distinct from that which follows collisional excitation of  $\text{SF}_6^-$ .

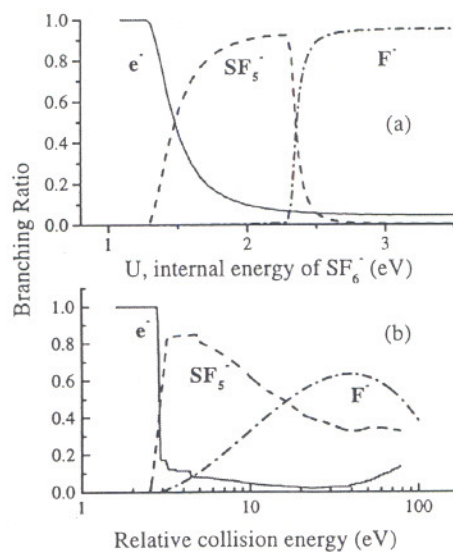


**Figure 2.** (a) Calculated branching ratios  $k_i^{\text{eff}}/(\sum k_i^{\text{eff}})$  as a function of  $U$ ; (b) Measured branching ratios  $\sigma_i/\sum(\sigma_i)$  as a function of  $E_{\text{rel}}$ .

## 4. SUMMARY

The target-independent features of collision-induced decomposition of  $SF_6^-$ , which has been observed for targets  $N_2$ , He, Ne, and Ar, can be qualitatively explained using a two-step model in which collisional decomposition is followed by unimolecular decomposition. This model shows that the dominance of CID processes result from the larger phase space for the CID channels than the electron detachment. The model calculation also suggests that the main source of  $F^-$  ions detected in collisions of  $SF_6^-$  with  $N_2$  may result from subsequent decomposition of excited  $SF_5^-$ .

## 5. ACKNOWLEDGMENTS

This work was supported in part by the U. S. Department of Energy, Office of Energy Science, Division of Chemical Sciences.

## 6. REFERENCES

- [1]. L.G. Christophorou and J.K. Olthoff, *J. Phys. Chem. Ref. Data*, **29**, 267 (2000).
- [2]. L.E. Kline, D.K. Davies, C.L. Chen, and P.J. Chantry, *J. Appl. Phys.* **50**, 6789 (1979).
- [3]. A. Chutjian and S. H. Alajian, *Phys. Rev. A* **31**, 1841 (1986).
- [4]. Y. Wang, R. L. Champion, L. D. Doverspike, J. K. Olthoff, and R. J. Van Brunt, *J. Chem. Phys.* **91**, 2254 (1989).
- [5]. L.G. Christophorou and R.J. Van Brunt, *IEEE Tran. Dielect. Electr. Insul.* **2**, 952 (1995).
- [6]. L.G. Christophorou, J.K. Olthoff and D.S. Green, "Gases for Electrical Insulation and Arc Interruption: Possible Present and Future Alternatives to Pure  $SF_6$ ," NIST Technical Note 1425 (1997).
- [7]. D. Smith, P. Spanel, S. Matejcik, A. Stamatovic, T.D. Mark, T. Jaffke, and E. Illenberger, *Chem. Phys. Lett.* **240**, 481 (1995).
- [8]. J.P. Astruc, R. Barbe, A. Lagreze, and J.P. Schermann, *Chem Phys.* **75**, 405 (1983).
- [9]. C.E. Klots, *J. Phys. Chem.* **75**, 1526 (1971); *J. Chem. Phys.* **64**, 4269 (1976).
- [10]. R.L.Champion, I.V. Dyakov, B.L. Peko, and Y. Wang, *J. Chem. Phys.*, submitted.
- [11]. S. E. Haywood, L. D. Doverspike, R. L. Champion, E. Herbst, B. K. Annis, and S. Datz, *J. Chem. Phys.* **74**, 2845 (1980).
- [12]. G.Z. Whitten and B.S. Rabinowitch, *J. Chem. Phys.* **41**, 1883 (1964).
- [13]. C.L. Lugez, M.E. Jacox, R.A. King, and H.F. Schaefer III, *J. Chem. Phys.* **108**, 9639 (1998).